Resisting the Effects of Aging: A Function for the Fiber Cell Beaded Filament

Kyoung-hye Yoon, **Tom Blankenship**, **Bradley Shibata**, **Paul G. FitzGerald**

Department of Cell Biology and Human Anatomy, School of Medicine, University of California, Davis, California.

Abstract

Purpose—The beaded filament is a cytoskeletal structure that has been found only in the lens fiber cell. It includes phakosin and filensin, two divergent members of the intermediate filament family of proteins that are also unique to the fiber cell. The authors sought to determine what function the beaded filament fulfills in the lens.

Methods—Light microscopy and electron microscopy were used to characterize structural changes that occurred in previously generated phakosin and filensin knockout mice. Immunocytochemistry and electron microscopy were used to define the distribution of phakosin, filensin, and beaded filaments.

Results—In phakosin and filensin knockout mice, initial lens development and the early phases of fiber cell differentiation proceed in a manner largely indistinguishable from that of wild type. Fiber cells elongate, undergo organelle elimination, and, in the organelle-free zone, develop the unique paddlelike extensions that characterize cells in this region. Subsequent to those stages, however, fiber cells undergo loss of the differentiated fiber cell phenotype and loss of the long-range stacking that characterizes fiber cells and that has been considered essential for clarity.

Conclusions—The beaded filament is not required for the generation of the differentiated fiber cell phenotype but is required to maintain that differentiated state and the long range order that characterizes the lens at the tissue level.

The family of intermediate filament (IF) proteins, with more than 60 members, is one of the largest in the human genome. Despite the large number of IF proteins available, a given cell typically uses three or fewer IF proteins in constructing its IF cytoskeleton. The IF proteins expressed by a given cell are strictly regulated by cell type and differentiation state.[1–5]

The lens expresses the type III IF protein vimentin in the lens epithelium and in the elongating fiber cells.[6–8] However, as fiber cell differentiation progresses, the expression of vimentin is downregulated, and expression of two new members of the IF family, phakosin and filensin, is turned on. These two proteins have thus far been demonstrated only in the

lens fiber cell and are considered among the most divergent members of the IF family. Notably, they are the only two cytoplasmic IF proteins that not found in the canonical 8 to 11 nm IF. Instead, they have been localized to a structure referred to as the beaded filament (BF).[9–20]

Knockout mice have been generated for phakosin and filensin.[21–23] Slit lamp examination of these knockouts suggests that the animals are born with optically clear lenses but that subtle light scattering in the deep cortex becomes detectable at approximately 3 weeks after birth, a scattering that becomes progressively worse with age. Examination of the optical properties of these knockout lenses was conducted using laser line tracing as well, further clarifying the perturbation of optical properties that occurs in these animals.[21] This study also suggested that structural changes occurred in the fiber cells somewhere in the deep cortex of older animals. Mutations in human phakosin have been implicated in inherited cataracts in at least two families. Paralleling the results achieved in the mouse knockout, lens changes in these affected family members were not reported until late childhood or early adult stages.[24,25]

To establish the structural basis for the loss of optical clarity observed in the BF null mice, we have characterized the structure of phakosin and filensin knockouts, as well as the double knockout, over a range of ages, correlating the structural changes to lens maturation and BF distribution. We concluded that the BF is not required for achievement of the highly differentiated state of the lens fiber cell but that it is required to sustain that differentiated fiber cell phenotype over time and to maintain the long-range and highly ordered stacking of fiber cells considered essential to optical clarity. The role of the BF in helping the fiber cell resist this time-dependent loss of normal lens architecture also explains why light scatter is not detected in the younger lenses but later grows to include progressively greater regions of the lens in older animals.

Materials and Methods

Tissue Processing

All animal procedures were conducted in accordance with ARVO Statement for the Use of Animals in Ophthalmic and Vision Research (located through the ARVO website at http://www.arvo.org) and the Declaration of Helsinki.

Scanning Electron Microscopy

For scanning electron microscopy mouse lenses were processed as described previously.[26] In brief, lenses were removed to GF fix (2.5% glutaraldehyde–2% formaldehyde in 0.1 M sodium cacodylate buffer), incubated for 30 minutes to 1 hour, then split in half along the anterior-posterior axis. Fixation was allowed to continue overnight. This process ensured fixative penetration throughout the entire lens. Tissues were dehydrated through acetone and critical point dried. Lenses were then split into quarters along the anterior-posterior axis, yielding a freshly fractured surface that exposed a complete lens radius. Specimens were sputter coated before examination with a scanning electron microscope (XL 30; Philips, Andover, MA).

Preparation of Lens Ghosts

Ghosted lenses were prepared as described previously,[27] with minor modifications. In brief, freshly enucleated mouse eyes were immersed in a conventional cryostat embedding medium (TES; Triangle Scientific, Raleigh, NC) and were frozen rapidly on dry ice. Lenses were stored at −80°C until used. Sections were cut on a cryostat (CM 3050; Leica, Wetzlar, Germany) at −15°C using the 150-μm setting on "trim" mode. To extract crystallins and reveal the underlying cytoskeleton, frozen sections were harvested in ice-cold PBS containing 5 mM EDTA and protease inhibitors (Complete Mini Protease Inhibitor; Roche Diagnostics, Basel, Switzerland) in a 70-mm Petri dish. Sections were agitated gently by orbital rotation on ice. The medium was changed twice over a 2-hour period to remove embedding medium and to extract soluble lens proteins. These sections are referred to as "lens ghosts." Ghosted sections were fixed in 2% paraformaldehyde for immunocytochemistry or GF fix for electron microscopy. Alternatively, to minimize crystallin extraction, some frozen sections were harvested directly into paraformaldehyde.

Immunocytochemistry

Ghost and nonghost frozen lens sections were fixed in 2% paraformaldehyde in 0.1 M phosphate buffer overnight, dehydrated through 100% ethanol, equilibrated in 100% xylene, and embedded in paraffin. Sections were cut and mounted on slides (Superfrost; Menzel-Glaser, Braunschsweig, Germany), deparaffinized, and rehydrated. Sections were "blocked" with 5% normal goat serum and 0.1% Tween 20 in PBS for 15 minutes. Primary antibody consisting of affinity-purified rabbit antibodies raised against recombinant mouse phakosin were diluted in blocker and overlaid on sections for 1 hour. After three large volume washes, at 10 minutes each, sections were reblocked, probed with biotinylated goat anti–rabbit antibodies, and incubated with streptavidin-labeled horseradish peroxidase, as described previously.[28]

Transmission Electron Microscopy

Some ghosted lens sections were fixed in 4% paraformaldehyde in 0.1 M phosphate buffer overnight, then split along the mid-coronal axis. One half was processed into paraffin as described. The matching half was postfixed in 1% osmium tetroxide for 1 hour and processed conventionally into epoxy resin for preparation of thin sections. Sections were stained with uranyl acetate and lead citrate and examined at 80 kV in a transmission electron microscope (CM 120; Philips).

Results

Structural Changes Caused by an Absence of BFs

Recently, the maturation of a structurally elaborate specialization that appears on the lateral edges of fiber cells was described in the mouse.[26] This process has also been described in previous studies as "paddle-like extensions" "hands" or "flaps" (for a spectacular image of these processes in fish lens, see Kuszak et al.[29]). These flaps emerge on lens fiber cells at about the time when organelles are lost, and continue to develop well into the organelle-free zone (OFZ). Developmental studies have shown that these flaps are not synthesized in fiber

cells "born" earlier than 2 to 3 postnatal weeks and thus are never present in the center of the mature lens. Cells born at successively later dates show increasingly well-developed flaps. Figure 1a shows a 1-month-old, wild-type lens as a baseline for comparison with the knockout. The view spans from the surface near the lens bow (left), to the nucleus. Even at this very low magnification, the zone of flaps is evident (white bar). These elaborations are most evident in the bow region, and they taper in magnitude toward either end of the fiber cell. Deep to this region are fiber cells born before the 2- to 3-week postnatal period, which never form the flaps. Thus, the fiber cells exhibiting the flap structures give way to fiber cells with simpler shapes and which show the highly ordered stacking that characterizes the wild-type lens. This regularity in fiber cell shape and stacking extends into the lens primary fiber cells, which are much less ordered. The boxed region in Figure 1a is presented at higher magnification in the inset, showing the exceptional degree of order in fiber cell stacking. The black arrow marks a point approximately 200 μm deep, which is compared to a similar region in the knockout.

Figure 1 also shows a 1-month-old phakosin knockout lens. At lower magnification (Fig. 1b), it is evident that the flap structures form (region overlaid by white bar) and that long-range order is exhibited in the fiber cells. This uniformity in fiber cell shape and stacking is evident up to approximately the 200-μm point (black arrow). Just deep to the 200-μm point is a relatively abrupt transition, where the uniform fiber cell shape and the ordered stacking are lost. At higher magnification (Fig. 1c), the loss of the regular, flattened-hexagon shape of the fiber cell is more clearly depicted. Individual cells are irregular and variable in shape, and the uniformity in fiber cell stacking seen in the Figure 1a inset is clearly lost. We have observed, as well, that the knockout lens was distinctly more fragile than the wild-type lens, noted both in the splitting of the lens for SEM and in the handling of thick, ghosted sections. The knockout frequently showed many fracture planes or splits in the tissue (see, for example, Fig. 1b) that were infrequent in the wild type, reflecting an overall higher level of fragility in the lens.

To determine the age at which fiber cells first exhibit the consequences of BF absence, we examined a series of knockout lenses ranging from 2 weeks of age to 7.5 months of age.

Two-week-old wild-type lenses (Fig. 2a) do not assemble the flap structures, and the uniform fiber cell shape and highly ordered stacking are evident all the way into the region of the primary lens fibers. Figure 2b is a slightly higher magnification view, but of a phakosin knockout showing the same regional loss of fiber cell shape and long range fiber cell stacking that was seen in the 1-month knockout lens. Thus, the absence of BFs is manifested at least as early as 2 weeks of age, before the detection of slit lamp anomalies. The emergence of structural changes occurs at about the halfway point between the surface and the lens center.

Figure 3a is a lower magnification overview that displays the outer cortical region of a 7.5-month knockout lens. A zone of flap structures is evident. However, these abruptly transition into the irregularly shaped fiber cells and tissue-level disorganization that characterizes the knockout phenotype (arrow). An example of this transition is shown at higher magnification in Figure 3b. This loss of fiber cell shape and stacking contrasts sharply with the 7.5-month

wild type (Fig. 3c), which shows the much larger extent of the flap zone in the wild-type lens, and the manner in which it transitions smoothly into uniformly shaped and well-stacked fiber cells of the deep cortex. Figure 3d is a higher magnification view of the wild-type lens that depicts the gradual transition from the elaborate flap zone (top) to more simplified fiber cell architecture and how the wild-type fiber cells maintain their precise stacking deep into the cortex. Thus, in the older knockout lens, the absence of BFs is manifested in what should have been the middle of the flap zone, eliminating the gradual transition back to the simpler fiber cell architecture seen in the wild type. As a result, the impacted area in the older knockout occupies a much greater percentage of lens volume than in the younger knockout. This likely accounts for the increased severity of the light scatter seen by slit lamp examination in the older animal.

Correlation of BF Distribution with Structural Changes Seen by SEM

In mouse lenses fixed by immersion in paraformaldehyde, immunolabeling of BF proteins showed a progressive increase as fiber cells differentiated, followed by a precipitous drop in labeling at about the time that organelles are dismantled (Fig. 4a). This pattern suggested that the BFs might not be present in the OFZ, where the impact of BF knockouts was most evident. The apparent absence of BFs in the very zone where fiber cell architecture is altered in the knockout complicated speculation about the role of BFs in stabilizing fiber cell shape. For this reason, we examined the status of BFs as a function of fiber cell birth date, examining cells deep into the OFZ for the presence or absence of BFs.

The very high concentration of cytoplasmic crystallins makes it difficult to identify BFs in conventionally processed tissue. To get around this, we examined "ghosts" of fiber cells, created by harvesting thick (150-μm) frozen sections into buffer, which allowed soluble crystallins to diffuse away. This methodology clearly reveals the underlying cytoskeleton. A cross-section of such a ghosted thick section is shown in Figure 4b, which is stained with toluidine blue. The lens capsule (arrow) in such a preparation tends to curl up, distorting the bow region, but the nuclei of the fiber cells located in the bow region are evident. The crystallins of the cortex in the mouse lens are soluble and readily extracted, resulting in a very pale staining of the cortical region. In contrast, the crystallins of the nuclear region are not as readily extracted, and they stain intensely (right-hand part of the section). An electron micrograph taken from the region boxed in Figure 4b, at the cortexnuclear boundary, and far removed from the deepest nucleated fiber cell, is shown in Figures 4c–d. The transition from the well-extracted fiber cells of the cortex (at the left) to less well-extracted cells of the nucleus (at the right) is evident as an increase in cytoplasmic density. At higher magnification (Fig. 4d), these fiber cells can be seen to have a rich BF cytoskeleton criss-crossing the cytoplasm. The identity of these BFs is confirmed in Figure 4g, by immunogold labeling of the frozen section with antibodies to BF proteins. Thus, BFs are clearly present in regions that are not immunoreactive in Figure 4a.

We envisioned two possible explanations for the absence of immunoreactivity seen in regions rich in BFs. First, phakosin and filensin experienced proteolytic damage with age, leaving the BF structurally intact but eliminating epitopes targeted by these antibodies. Second, fixation of the deeper cortex, where crystallin density is higher than superficial

cortex, produced a barrier to antibody penetration, masking epitopes, a phenomenon noted by Beebe et al.[30]

To test this, we compared the relative immunoreactivity of frozen sections that had been extracted with buffer to remove soluble crystallins (Fig. 4e) with those that had been fixed immediately in paraformaldehyde (Fig. 4f) to minimize the extraction of crystallins. These sections were then embedded in paraffin and sectioned for immunocytochemistry. Figure 4e, where crystallins had been extracted, shows very intense pha-kosin labeling all the way through to the nuclear-cortical boundary (brown reaction product). In contrast, sections that were fixed immediately showed heavy labeling only in the outer cortex, where crystallin density was low, and at the immediate surface of the section, where some diffusion occurred when sections were placed in fixative (Fig. 4f). (Only one surface is labeled because the sections floated.) The heavily labeled region in the outer cortex (Fig. 4f) is similar in extent to the region labeled in immersion-fixed and conventionally-processed paraffin sections. From this we conclude that epitope loss is not the explanation for the absence of immunolabeling in paraffin sections because extracted sections label, and we conclude that crystallin blocking accounts for the disparity.

Collectively, the data in Figure 4 show that BFs are present in cells in which the knockout phenotype is manifested and that BFs in this region are critical to the maintenance of the fiber cell and lens phenotype.

Discussion

The data presented here establish that the function of the BF is to maintain the differentiated fiber cell phenotype and the long-range, highly ordered stacking of fiber cells, considered critical for optical clarity. The BF thereby maintains order at both the cellular and the tissue levels. Notably, the BF is not required to achieve these phenotypes, only to maintain them in older cells. This suggests that the differentiated phenotype of the lens is intrinsically unstable and prone to randomization and that BFs retard the innate propensity of fiber cell and lens structure to randomize.

These data establish, also, that the BFs serve this function throughout the entire cortex, well past the point at which organelles are lost and at least until the cortex-nucleus boundary, as suggested by Sandilands et al.[21] The high degree of insolubility of mouse lens nuclear crystallins precluded extending these observations to the nucleus.

In lenses of younger knockouts, the loss of fiber cell structure was manifested deep in the cortex, whereas in the older lenses the affected zone was seen relatively closer to the surface and much closer to the region of nucleated fiber cells. The general shape and size of the affected area, and its progression from a smaller fraction of the central lens volume to a relatively greater fraction that is seen closer to the lens surface, mirror the slit lamps findings noted in the original knockout characterizations.[22,23,31] Thus, the impacted region occupies a relatively much greater volume of the older lens. One explanation for this may be that the rate of growth in younger lenses is much faster than in older lenses. Cells that require a

specific time period before they manifest a breakdown in structure will be buried deeper in a faster growing lens than in a slower growing lens.

We also note that BF knockout lenses were distinctly more fragile that the wild-type lenses in macroscopic procedures. Whole lenses were less resilient, whereas ghosted sections readily fell apart. Given the absence of any other cytoskeletal elements in the cortical fiber cells, an increased susceptibility to mechanical trauma might be predicted.

That the BF is required to maintain the differentiated phenotype but not to achieve it mirrors the role of IFs in other tissues. Skin, for example, differentiates normally in the absence of specific epidermal keratins but will be exceptionally susceptible to mechanical trauma.[32–39] Why the lens requires two fiber cell-specific proteins to accomplish this task is unclear. We can speculate that the necessary linkages between cytoskeleton and membrane must be tailored to the constellation of membrane proteins expressed in that differentiated cell.

This would be consistent with the observation that BF proteins are able to bind MIP, a dominant, fiber cell-specific membrane protein.[40] Alternatively, the BF proteins may exhibit a high degree of resistance to proteolysis, a resistance that represents a desirable trait in a cell that lacks the capacity for turnover and replacement of proteins.

We also note here that conventional immersion fixation of lenses may yield misleading results in immunocytochemical procedures. We show that otherwise robust antigens can be masked to the point of undetectability in the deeper cortex, where crystallin density is very high, while yielding a vigorous signal in the outer cortex, where crystallin density is much lower. Aldehyde fixation of the very dense crystallins appears to create a physical barrier that antibodies cannot penetrate. This mirrors the results achieved by Beebe et al.,[30] who established epitope masking of N-cadherin and band 4.1 labeling in fixed lens sections that was unmasked by previous treatment with detergent.

Acknowledgments

References

1. Albers K, Fuchs E. The molecular biology of intermediate filament proteins. Int Rev Cytol. 1992;134:243–279. [PubMed: 1374743]

2. Coulombe PA, Ma L, Yamada S, Wawersik M. Intermediate filaments at a glance. J Cell Sci. 2001;114:4345–4347. [PubMed: 11792800]

3. Fuchs E, Weber K. Intermediate filaments: structure, dynamics,function, and disease. Annu Rev Biochem. 1994;63:345–382. [PubMed: 7979242]

4. Goldman RD, Steinert PM. Cellular and Molecular Biology of Intermediate Filaments. New York, NY: Plenum Press; 1990.

5. Herrmann HAH Jr. Intermediate Filaments. New York: Plenum; 1998.

6. Bagchi M, Caporale MJ, Wechter RS, Maisel H. Vimentin synthesis by ocular lens cells. Exp Eye Res. 1985;40:385–392. [PubMed: 4065233]

7. Ellis M, Alousi S, Lawniczak J, Maisel H, Welsh M. Studies on lens vimentin. Exp Eye Res. 1984;38:195–202. [PubMed: 6370709]

8. Bloemendal H, Benedetti EL, Ramaekers F, Dunia I. The lens cytoskeleton: intermediate-sized filaments, their biosynthesis and association with plasma membranes. Mol Biol Rep. 1981;7:167–168. [PubMed: 7195979]

9. Remington SG. Chicken filensin: a lens fiber cell protein that exhibits sequence similarity to intermediate filament proteins. J Cell Sci. 1993;105:1057–1068. [PubMed: 7693735]

10. Ireland M, Maisel H. A family of lens fiber cell specific proteins. Lens Eye Toxic Res. 1989;6:623–638. [PubMed: 2487275]

11. Ireland M, Maisel H. A cytoskeletal protein unique to lens fiber cell differentiation. Exp Eye Res. 1984;38:637–645. [PubMed: 6381079]

12. Sandilands A, Prescott AR, Carter JM et al. Vimentin and CP49/filensin form distinct networks in the lens which are independently modulated during lens fibre cell differentiation. J Cell Sci. 1995;108:1397–1406. [PubMed: 7615661]

13. FitzGerald PG, Graham D. Ultrastructural localization of alpha A-crystallin to the bovine lens fiber cell cytoskeleton. Curr Eye Res. 1991;10:417–436. [PubMed: 1889228]

14. FitzGerald PG. Immunochemical characterization of an M_r 115 lens fiber cell-specific extrinsic membrane protein. Curr Eye Res. 1988; 7:1243–1253. [PubMed: 3229135]

15. Hess JF, Casselman JT, FitzGerald PG. Gene structure and cDNA sequence identify the beaded filament protein CP49 as a highly divergent type I intermediate filament protein. J Biol Chem. 1996; 271:6729–6735. [PubMed: 8636093]

16. Hess JF, Casselman JT, FitzGerald PG. cDNA analysis of the 49 kDa lens fiber cell cytoskeletal protein: a new, lens-specific member of the intermediate filament family? Curr Eye Res. 1993;12:77–88. [PubMed: 7679620]

17. Gounari F, Merdes A, Quinlan R, et al. Bovine filensin possesses primary and secondary structure similarity to intermediate filament proteins. J Cell Biol. 1993;121:847–853. [PubMed: 8491777]

18. FitzGerald PG, Gottlieb W. The M_r 115 kd fiber cell-specific protein is a component of the lens cytoskeleton. Curr Eye Res. 1989;8:801–811. [PubMed: 2791627]

19. Sawada K, Agata J, Eguchi G, Quinlan R, Maisel H. The predicted structure of chick lens CP49 and a variant there of, CP49ins, the first vertebrate cytoplasmic intermediate filament protein with a lamin-like insertion in helix 1B. Curr Eye Res. 1995;14:545–553. [PubMed: 7587300]

20. Masaki S, Quinlan RA. Gene structure and sequence comparisons of the eye lens specific protein, filensin, from rat and mouse: implications for protein classification and assembly. Gene. 1997; 201:11–20. [PubMed: 9409766]

21. Sandilands A, Prescott AR, Wegener A, et al. Knockout of the intermediate filament protein CP49 destabilises the lens fibre cell cytoskeleton and decreases lens optical quality, but does not induce cataract. Exp Eye Res. 2003;76:385–391. [PubMed: 12573667]

22. Alizadeh A, Clark JI, Seeberger T, et al. Targeted genomic deletion of the lens-specific intermediate filament protein CP49. Invest Ophthalmol Vis Sci. 2002;43:3722–3727. [PubMed: 12454043]

23. Alizadeh A, Clark J, Seeberger T, Hess J, Blankenship T, FitzGerald PG. Targeted deletion of the lens fiber cell-specific intermediate filament protein filensin. Invest Ophthalmol Vis Sci. 2003;44: 5252–5258. [PubMed: 14638724]

24. Jakobs PM, Hess JF, FitzGerald PG, Kramer P, Weleber RG, Litt M.Autosomal-dominant congenital cataract associated with a deletion mutation in the human beaded filament protein gene BFSP2 [In Process Citation]. Am J Hum Genet. 2000;66:1432–1436. [PubMed: 10739768]

25. Grimes PA, Favor J, Koeberlein B, Silvers WK, Fitzgerald PG, Stambolian D. Lens development in a dominant X-linked congenital cataract of the mouse. Exp Eye Res. 1993;57:587–594. [PubMed: 8282045]

26. Blankenship T, Bradshaw L, Shibata B, Fitzgerald P. Structural specializations emerging late in mouse lens fiber cell differentiation. Invest Ophthalmol Vis Sci. 2007;48:3269–3276. [PubMed: 17591898]

27. FitzGerald PG. Methods for the circumvention of problems associated with the study of the ocular lens plasma membrane-cytoskeleton complex. Curr Eye Res. 1990;9:1083–1097. [PubMed: 2095320]

28. Blankenship TN, Hess JF, FitzGerald PG. Development- and differentiation-dependent reorganization of intermediate filaments in fiber cells. Invest Ophthalmol Vis Sci. 2001;42:735–742. [PubMed: 11222535]

29. Kuszak JR, Peterson KL, Brown HG. Electron microscopic observations of the crystalline lens. Microsc Res Tech. 1996;33:441–479. [PubMed: 8800752]

30. Beebe DC, Vasiliev O, Guo J, Shui YB, Bassnett S. Changes in adhesion complexes define stages in the differentiation of lens fiber cells. Invest Ophthalmol Vis Sci. 2001;42:727–734. [PubMed: 11222534]

31. Alizadeh A, Clark J, Seeberger T, Hess J, Blankenship T, FitzGerald PG. Characterization of a mutation in the lens-specific CP49 in the 129 strain of mouse. Invest Ophthalmol Vis Sci. 2004;45:884–891. [PubMed: 14985306]

32. Coulombe PA, Fuchs E. Epidermolysis bullosa simplex. Semin Dermatol. 1993;12:173–190. [PubMed: 7692916]

33. Coulombe PA, Hutton ME, Letai A, Hebert A, Paller AS, Fuchs E. Point mutations in human keratin 14 genes of epidermolysis bullosa simplex patients: genetic and functional analyses. Cell. 1991; 66:1301–1311. [PubMed: 1717157]

34. Coulombe PA, Hutton ME, Vassar R, Fuchs E. A function for keratins and a common thread among different types of epidermolysis bullosa simplex diseases. J Cell Biol. 1991;115:1661–1674. [PubMed: 1721910]

35. Fuchs E Epidermal differentiation: the bare essentials. J Cell Biol. 1990;111:2807–2814. [PubMed: 2269655]

36. Fuchs E Keratin genes, epidermal differentiation and animal models for the study of human skin diseases. Biochem Soc Trans. 1991;19:1112–1115. [PubMed: 1724430]

37. Fuchs E Intermediate filaments and disease: mutations that cripple cell strength. J Cell Biol. 1994;125:511–516. [PubMed: 7513705]

38. Fuchs E, Cleveland DW. A structural scaffolding of intermediate filaments in health and disease. Science. 1998;279:514–519. [PubMed: 9438837]

39. Fuchs E, Coulombe P, Cheng J, et al. Genetic bases of epidermolysis bullosa simplex and epidermolytic hyperkeratosis. J Invest Dermatol 1994;103:25S–30S. [PubMed: 7525738]

40. Fan J, Fariss RN, Purkiss AG, et al. Specific interaction between lens MIP/Aquaporin-0 and two members of the gamma-crystallin family. Mol Vis. 2005;11:76–87. [PubMed: 15692460]
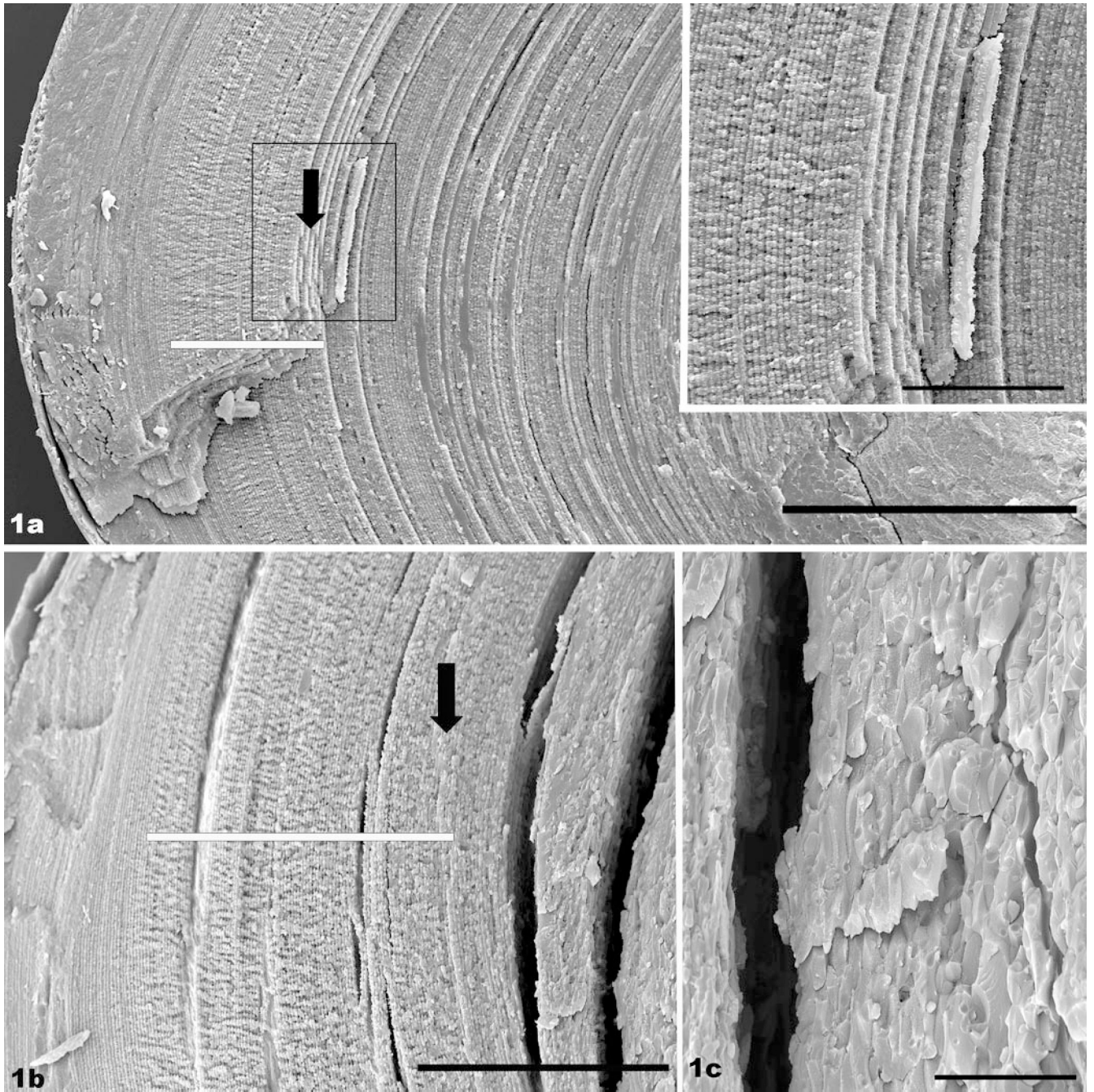
FIGURE 1.

(**a**) SEM of a 1-month-old, wild-type mouse lens. The view spans from the lens surface at the bow region (*left*) to the lens nucleus (*right*). The region in which the handlike structures are evident is highlighted by the *white bar*. The fiber cells deep to this region maintain a uniform and regular shape and are precisely aligned and stacked, showing a high degree of long-range order. A point approximately 200 μm into the lens is indicated by the *black arrow*. *Inset*: higher magnification view of the region boxed in (**a**). (**b**) SEM of a 1-month-old phakosin knockout lens. The "hand" region is highlighted by the *white bar*. A point

approximately 200 μm from the surface is marked by the *arrow*. The first evidence of a loss of fiber cell structure caused by the absence of the BF occurs just to the right of the *arrow*, close to where the split occurs in this more fragile tissue. (**c**) SEM of a 1-month-old phakosin knockout lens, in the region exhibiting a loss of fiber cell shape and fiber cell stacking. Scale bar: (**a**) 200 μm; (*inset*) 50 μm; (**b**) 100 μm; (**c**) 20 μm.
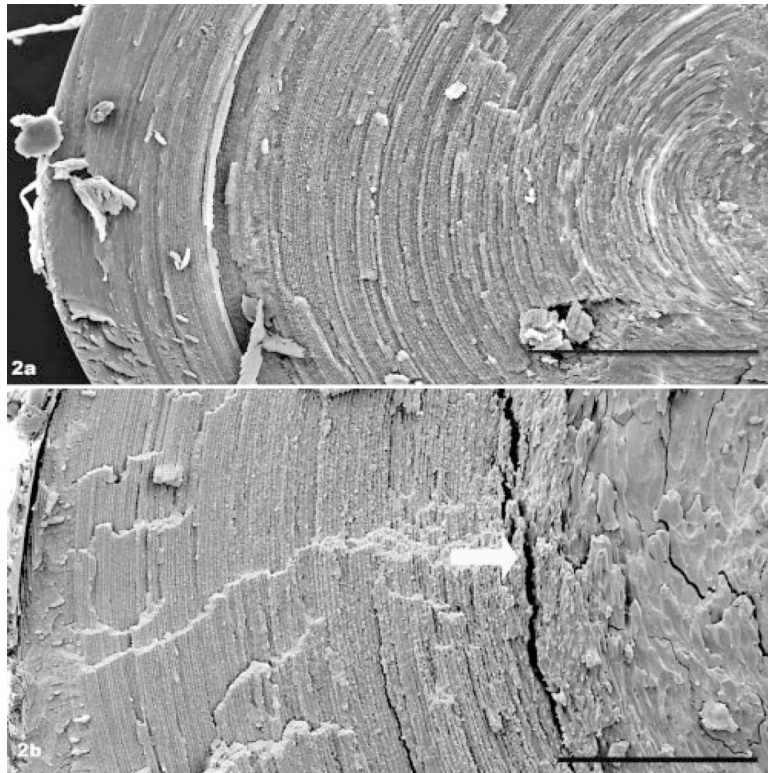
FIGURE 2.
(**a**) SEM of 2-week-old, wild-type lens, spanning from the surface at the bow region (*left*) to the nucleus (*right*). (**b**) Slightly higher magnification SEM of 2-week-old phakosin knockout lens, spanning from the bow region to the deep cortex. The loss of long-range order of fiber cells becomes evident in the deep cortex, at approximately the *white arrow*. Scale bar: (**a**) 200 μm; (**b**) 100 μm.
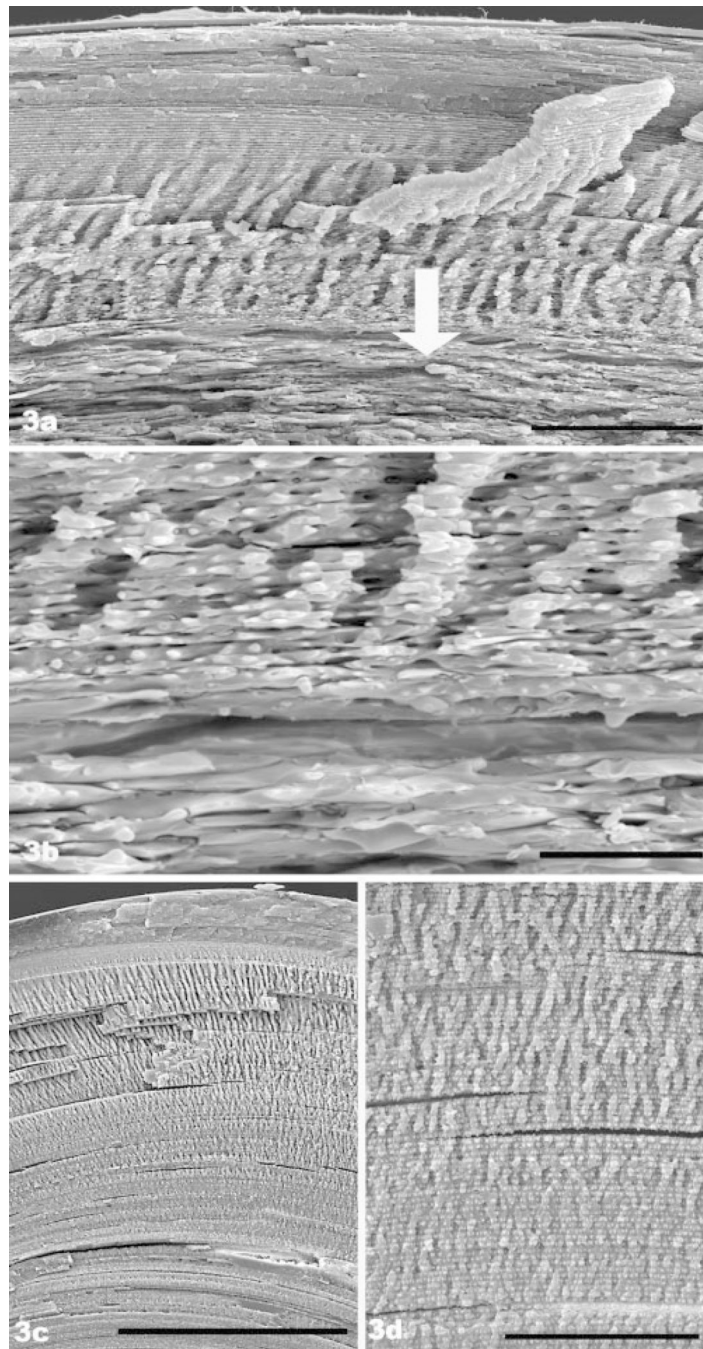
FIGURE 3.

(**a**) SEM of 7.5-month-old filensin knockout. The lens surface at the bow region is located at the *top*. The most superficial region of the "hand" zone is evident. However, the loss of structure caused by the absence of beaded filaments begins a short way into the hand zone (*arrow*), greatly reducing its domain (compare with Fig. 4b of wild type). (**b**) Higher magnification SEM view of the region, where the impact of BF absence first becomes evident in the 7.5-month-old knockout (a region comparable to the area overlaid by the arrow in Fig. 3a). (**c**) SEM overview of 7.5-month-old wild-type lens, showing the normal,

much larger extent of the hand domain. Black bar, 200 μm. In contrast to (**a**), the long-range, highly ordered stacking of fiber cells is evident well into the deep cortex. (**c**) Higher magnification view of the deep cortex of the 7.5-month-old wild-type lens, showing the gradual transition from the hand domain to deeper cortex. This contrasts with the abrupt loss of fiber cell shape and regular packing evident in the knockout (**a**, **b**). Scale bar: (**a**), 50 μm; (**b**) 10 μm; (**c**) 50 μm.
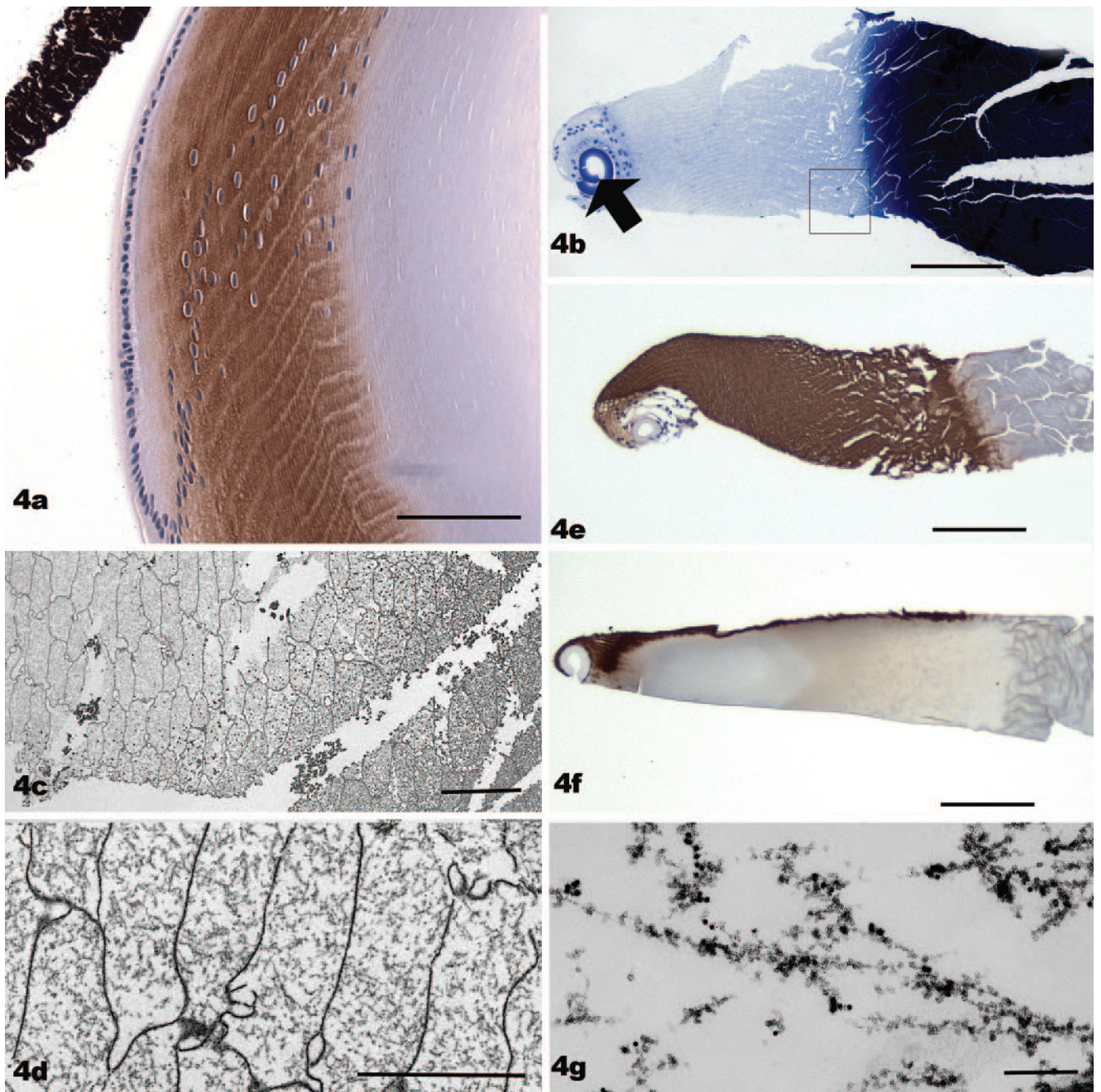
FIGURE 4.

(**a**) A paraffin section from a mouse lens fixed by conventional immersion fixation, then immunolabeled with antibodies to phakosin (brown reaction product). The reaction product is absent from the epithelium, very light in elongating fiber cells, and much more intense in the nucleated fiber cells. The immunoreactivity falls off abruptly at about the level where the fiber cell loses its organelles. Nuclei are stained blue with hematoxylin. (**b**) A paraffin section of a thick, "ghosted," frozen section, stained with toluidine blue. The curled capsule is evident as a *thick blue line* (*arrow*). Nuclei of differentiating fiber cells can be seen as well. The cortical region is very pale staining because of the absence of crystallins. In

contrast, the nuclear region, where crystallins are much less soluble, stains an intense blue black. (**c**) An electron micrograph of a thick, ghosted, frozen section, near the corticonuclear interface, similar in orientation to (**b**), (**e**), and (**f**). The more extracted fiber cells of the cortical region present as flattened hexagons, characteristic of cross-sectioned fiber cells. (**d**) Higher magnification view of a region of cortex from a thick, ghosted, frozen section. The degree to which the BFs dominate the cytoplasm is evident in the absence of crystallins. (**e**) Paraffin section of a thick, ghosted, frozen section, comparable to that seen in (**b**). However, this section is immunolabeled with antibodies to phakosin (brown reaction product). This section has not been stained with toluidine blue. Note that the entire cortex is intensely immunoreactive when crystallins have been extracted. (**f**) A paraffin section of a thick, ghosted, frozen section, immunolabeled with antibodies to phakosin (brown reaction product). However, in this case, the section was harvested directly into fixative to minimize the extraction of crystallins. Immunolabeling is confined to the surface of the section, where some crystallin diffusion occurred on immersion in fixative. The superficial cortex, where fiber cells are elongating and are not yet filled with crystallins, is also stained. It is clear that fixation in the presence of crystallins can create a barrier to antigen-antibody interaction. (**g**) Electron micrograph of a thick, ghosted, frozen section, labeled with antiphakosin and filensin, and colloidal gold secondary antibodies before fixation. This view is within a single fiber cell cytoplasm and confirms the identity of the cytoskeletal structures seen in (**c**) and (**d**) as BFs. Scale bar: (**a**) 60 μm; (**b**, **e**, **f**) 115 μm; (**c**) 10 μm; (**d**) 5 μm; (**g**) 160 nm.